

# North Carolina Macular Dystrophy: Phenotypic Variability and Computational Analysis of Disease-Associated Noncoding Variants

David J. Green,<sup>1</sup> Eva Lenassi,<sup>1-3</sup> Cerys S. Manning,<sup>4</sup> David McGaughey,<sup>5</sup> Vinod Sharma,<sup>3</sup> Graeme C. Black,<sup>1,2</sup> Jamie M. Ellingford,<sup>1</sup> and Panagiotis I. Sergouniotis<sup>1-3,6</sup>

<sup>1</sup>Division of Evolution and Genomic Sciences, School of Biological Sciences, Faculty of Biology, Medicine and Health, University of Manchester, Manchester, United Kingdom

<sup>2</sup>Manchester Centre for Genomic Medicine, St Mary's Hospital, Manchester University NHS Foundation Trust, Manchester, United Kingdom

<sup>3</sup>Manchester Royal Eye Hospital, Manchester University NHS Foundation Trust, Manchester, United Kingdom

<sup>4</sup>Division of Developmental Biology and Medicine, School of Medical Sciences, Faculty of Biology, Medicine and Health, University of Manchester, Manchester, United Kingdom

<sup>5</sup>Ophthalmic Genetics and Visual Function Branch, National Eye Institute, National Institutes of Health, Bethesda, Maryland, United States

<sup>6</sup>Institute of Biochemistry and Molecular Genetics, Faculty of Medicine, University of Ljubljana, Ljubljana, Slovenia

Correspondence: Panagiotis I. Sergouniotis FRCOphth, Manchester Centre for Genomic Medicine, St Mary's Hospital, Oxford Road, Manchester M13 9WL, UK; [panagiotis.sergouniotis@manchester.ac.uk](mailto:panagiotis.sergouniotis@manchester.ac.uk).

DJG and EL contributed equally to the work and should therefore be regarded as equivalent first authors.

**Received:** December 23, 2020

**Accepted:** May 12, 2021

**Published:** June 14, 2021

Citation: Green DJ, Lenassi E, Manning CS, et al. North Carolina macular dystrophy: Phenotypic variability and computational analysis of disease-associated noncoding variants. *Invest Ophthalmol Vis Sci.* 2021;62(7):16. <https://doi.org/10.1167/iovs.62.7.16>

**PURPOSE.** North Carolina macular dystrophy (NCMD) is an autosomal dominant, congenital disorder affecting the central retina. Here, we report clinical and genetic findings in three families segregating NCMD and use epigenomic datasets from human tissues to gain insights into the effect of NCMD-implicated variants.

**METHODS.** Clinical assessment and genetic testing were performed. Publicly available transcriptomic and epigenomic datasets were analyzed and the activity-by-contact method for scoring enhancer elements and linking them to target genes was used.

**RESULTS.** A previously described, heterozygous, noncoding variant upstream of the *PRDM13* gene was detected in all six affected study participants (chr6:100,040,987G>C [GRCh37/hg19]). Interfamilial and intrafamilial variability were observed; the visual acuity ranged from 0.0 to 1.6 LogMAR and fundoscopic findings ranged from visually insignificant, confluent, drusen-like macular deposits to coloboma-like macular lesions. Variable degrees of peripheral retinal spots (which were easily detected on widefield retinal imaging) were observed in all study subjects. Notably, a 6-year-old patient developed choroidal neovascularization and required treatment with intravitreal bevacizumab injections. Computational analysis of the five single nucleotide variants that have been implicated in NCMD revealed that these noncoding changes lie within two putative enhancer elements; these elements are predicted to interact with *PRDM13* in the developing human retina. *PRDM13* was found to be expressed in the fetal retina, with greatest expression in the amacrine precursor cell population.

**CONCLUSIONS.** We provide further evidence supporting the role of *PRDM13* dysregulation in the pathogenesis of NCMD and highlight the usefulness of widefield retinal imaging in individuals suspected to have this condition.

**Keywords:** north carolina macular dystrophy, noncoding variation, gene regulatory network, transcriptional enhancer, widefield retinal imaging

North Carolina macular dystrophy (NCMD) is a developmental abnormality affecting the macula, the central part of the retina that is responsible for detailed vision. NCMD is present at birth and rarely progresses. It is inherited as an autosomal dominant trait and although it is thought to be completely penetrant, it exhibits significant intrafamilial and interfamilial variability. The phenotype ranges from visually inconsequential subtle retinal spots to macular coloboma-like lesions that may be associated with significant visual impairment.<sup>1-6</sup>

NCMD was first described in the 1970s in a large pedigree of more than 500 individuals spanning seven generations. This kindred represented a portion of the descendants of two brothers who emigrated from Ireland to the mountains of North Carolina in the early nineteenth century.<sup>7,8</sup> Since the first description of the disease, families have been reported in Europe, North America, Asia, and elsewhere in the world (suggesting that the term NCMD is a misnomer).<sup>9-14</sup> NCMD is genetically heterogeneous, but most individuals carry genetic variants in an intragenic region in

chromosome 6 located approximately 13,000 base-pairs from the neighboring gene. At least five single nucleotide changes and three copy number variants in this region have been associated with NCMD.<sup>1,3,4,9,15</sup> These mutations alter DNA sequences that are likely to play a role in regulating the spatiotemporal expression of a retinal transcription factor *PRDM13*. *PRDM13* is expressed in the fetal retina, but is not found in adult tissues.<sup>1</sup> Overexpression of this gene has been shown to affect retinal development in nonprimate animal models.<sup>16</sup> Intriguingly, changes near *PRDM13* that have been associated with NCMD have also been implicated in a different condition, progressive bifocal chorioretinal atrophy (PBCRA). Although both of these disorders affect the macula from birth, the latter is typically associated with disease progression and electrophysiologic evidence of widespread retinal dysfunction.<sup>2</sup> It is also noteworthy that a number of individuals with a phenotype indistinguishable from NCMD have been found to have copy number variants in a different locus in chromosome 5.<sup>1,2</sup>

NCMD is part of an expanding group of Mendelian conditions caused by noncoding genetic variants that have an effect on gene expression (e.g., aniridia,<sup>17</sup> limb malformations<sup>18</sup>). These variants often alter the sequence of regulatory elements, including transcriptional promoters and enhancers. Enhancers are short stretches of DNA, typically a few hundred base-pairs long, that bind transcription factors and enhance the expression of specific genes.<sup>19</sup> There are hundreds of thousands of enhancers in the human genome but our understanding of their properties and repertoire is limited (e.g., where they reside, what genes they mediate their effects through, in which cells and in which specific time of development they act). Notably, our ability to detect and annotate enhancer elements is being transformed by emerging resources and tools such as the Encyclopedia of DNA Elements (ENCODE) 3 dataset,<sup>20</sup> the Developmental Single Cell Atlas of Gene Regulation and Expression (DESCARTES),<sup>21,22</sup> and the activity-by-contact (ABC) model.<sup>23,24</sup> The ENCODE project consortium and the DESCARTES team have generated extensive functional genomic datasets across many cell and tissue contexts. Experiments conducted include assays aiming to identify enhancer elements such as DNase-seq (DNase I hypersensitive site sequencing), H3K27ac ChIP-seq (chromatin immunoprecipitation sequencing mapping H3K27 acetylation signals), and ATAC-seq (assay for transposase-accessible chromatin using sequencing), as well as assays studying the 3-dimensional architecture of the genome such as Hi-C (all-versus-all chromosome conformation capture).<sup>20–22</sup> ABC, in contrast, is a method that uses these epigenomic data to predict which enhancers regulate which genes. This model is based on the notion that an enhancer's effect on a gene depends on the enhancer's strength (estimated using chromatin accessibility data including ATAC-seq and H3K27ac ChIP-seq data) weighted by how often it comes into three-dimensional contact with the gene promoter (estimated using Hi-C data).<sup>23,24</sup> Although this method has been shown to be accurate, a limiting factor is the availability of tissue-specific chromatin accessibility datasets. Comprehensive tissue-specific Hi-C data are also lacking, but the developers of ABC expect that Hi-C profiles averaged across a selection of cell types are adequate to map enhancer–gene connections. However, it remains possible that tissue- and context-specific data are required in some cases because the three-dimensional conformation of the genome shows some plasticity during development.<sup>25</sup> Although epigenomic

datasets from various eye tissues are becoming increasingly available,<sup>26</sup> there have been no systematic efforts to characterize enhancers that contribute to human vision.

In this report, we discuss phenotypic variability in individuals who have NCMD and are heterozygous for a specific noncoding variant, chr6:100,040,987G>C (GRCh37/hg19). We then use the ABC method and human transcriptomic and epigenomic datasets to gain mechanistic insights into the role of noncoding variation in NCMD.

## METHODS

### Participant Ascertainment, Phenotypic Data Collection, and Clinical Genetic Testing

Six individuals with a diagnosis of NCMD were retrospectively ascertained through the database of the North West Genomic Laboratory Hub, Manchester, UK. The study participants originated from three reportedly unrelated families who had European ancestries. The genetic and, to an extent, the clinical findings from two of the three affected individuals in one of these families have been reported previously.<sup>15</sup> Ethics committee approval for the study was obtained from the North West Research Ethics Committee (11/NW/0421 and 15/YH/0365) and all investigations were conducted in accordance to the tenets of the Declaration of Helsinki.

All study participants were diagnosed with NCMD through the tertiary ophthalmic genetics service at Manchester University NHS Foundation Trust, Manchester, UK. Clinical assessment included visual acuity testing, dilated fundus examination, digital widefield fundus imaging, fundus autofluorescence imaging, optical coherence tomography (OCT), and OCT-angiography (OCT-A). The Optos system (Optos PLC, Dunfermline, Scotland, UK) was used to obtain widefield images, the Topcon DRI OCT Triton device (Topcon GB, Newberry, Berkshire, UK) was used to obtain OCT and OCT-A scans, and the Spectralis system (Heidelberg Engineering, Heidelberg, Germany) was used to acquire fundus autofluorescence and OCT images in study participants.

Genetic testing was performed at the North West Genomic Laboratory Hub, a UK Accreditation Service (UKAS) Clinical Pathology Accredited (CPA) medical laboratory (CPA identifier, no. 4015). DNA samples from all study participants were screened using Sanger sequencing (BigDye v3.1) for the presence of known NCMD-associated variants in chromosome 6 (upstream of the *PRDM13* gene<sup>1</sup>). Two affected individuals also underwent genome sequencing as previously described (case 89794.1<sup>27</sup> and case 75898.2<sup>15</sup>) (Fig. 1 and Table 1); the generated data were used for haplotype analysis (Supplementary Table S1).

### Analysis of Variants Associated With NCMD

To gain insights into the frequency of NCMD-associated variants in the general population, we queried the Genome Aggregation Database (gnomAD; version 3.1) and the NHLBI Trans-Omics for Precision Medicine variant database (TOPMed; freeze 8). Neither of these cohorts is known to be enriched for patients with ophthalmic conditions.<sup>28,29</sup>

All variants known to be associated with NCMD (including the chr6:100,040,987G>C change detected in the study participants) were assessed using *in silico* tools that attempt to predict the deleteriousness of noncoding sequence

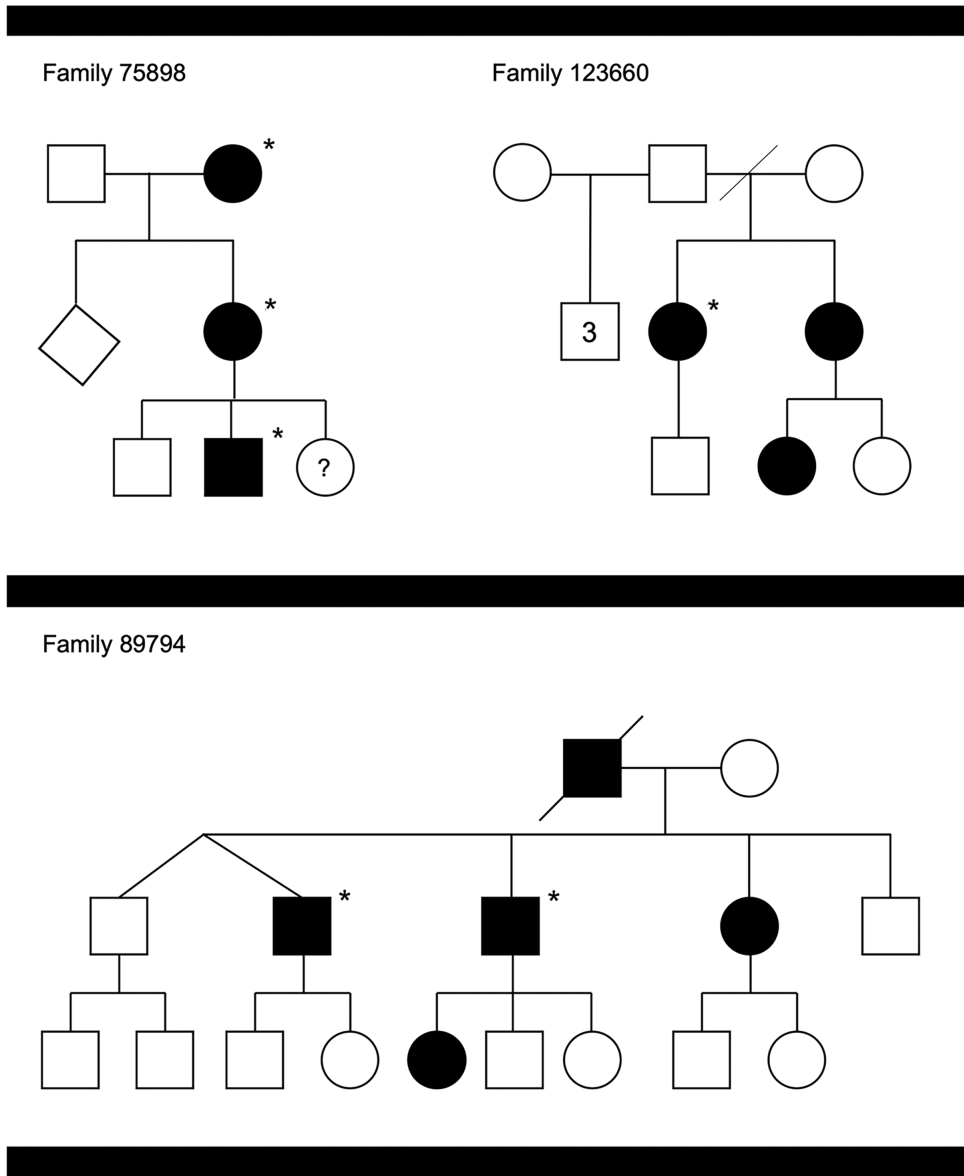


**FIGURE 1.** Pedigrees from three families segregating NCMD. Study participants are highlighted with asterisks. We note that findings from the two affected females from family 75898 are also discussed in.<sup>15</sup>

alterations. The following tools were used: CADD (Combined Annotation Dependent Depletion) v1.6,<sup>30</sup> nCER (NonCoding Essential Regulation) v2,<sup>31</sup> and regBase v1.1.<sup>32</sup> Position-specific evolutionary constraint was evaluated using GERP (Genomic Evolutionary Rate Profiling) scores<sup>33</sup> obtained through the University of California, Santa Cruz genome browser (available at: <https://genome.ucsc.edu/>).

To investigate the functional effects of the variants associated with NCMD, we queried the v109 release of the ENCODE portal for putative enhancer elements spanning the location of each variant; the SCREEN (Search Candidate cis-Regulatory Elements by ENCODE) v10 interface was used.<sup>20</sup> We also inspected the expression quantitative trait loci (eQTL) catalogue and the Genotype-Tissue Expression (GTEx) and Eye Genotype Expression (EyeGEx) datasets for eQTL overlapping any of the detected elements (in addition to elements predicted in our subsequent analyses).<sup>34,35</sup> We then queried the DESCARTES chromatin accessibility

database for the location of NCMD-associated variants across all available tissues.

The ABC method for scoring enhancer elements and linking them to target genes was subsequently used.<sup>23,24</sup> Raw ATAC-seq and H3K27ac ChIP-seq reads from macular and retinal tissue were obtained from a publicly available dataset (GEO accession: GSE137311).<sup>26</sup> The data were then processed using a consistent pipeline. The raw reads were trimmed for quality and adaptor content using the fastp tool with default quality control options.<sup>36</sup> The trimmed ATAC-seq and ChIP-seq reads were aligned to the GRCh37/hg19 reference sequence using bowtie2 version 2.3.0 with the default parameters.<sup>37</sup> The alignments were inspected in picard tools version 2.1.0 (<https://broadinstitute.github.io/picard/>) and duplicate reads were removed. Only reads with a mapping quality of 30 or higher were retained in subsequent analyses after filtration using the samtools “-view” command (version 1.9).<sup>38</sup>

**TABLE 1.** Clinical Characteristics of Individuals Carrying the chr6:100,040,987G>C (GRCh37/hg19) Change in Heterozygous State

Patient	Sex	Age (at Presentation; at Last Examination)	LogMAR Vision at Last Examination (Right; Left)	Main Fundoscopic Findings
75898.1	Male	3; 7	0.5; 1.6	Coloboma-like macular lesions; subfoveal scarring and fluid owing to neovascularization; subtle peripheral drusenoid lesions
75898.2	Female	4; 36	0.5; 0.5	Coloboma-like macular lesions with associated macular drusenoid lesions and a degree of foveal sparing; peripheral drusenoid lesions
75898.3	Female	4; 58	1.5; 1.5	Coloboma-like macular lesions with associated macular drusenoid lesions; peripheral drusenoid lesions
123660.1	Female	35; 37	0.0; 0.0	Macular and peripheral drusenoid lesions
89794.1	Male	44; 50	0.0; 0.0	Macular and peripheral drusenoid lesions
89794.2	Male	46; 52	0.0; 0.0	Macular and peripheral drusenoid lesions

Patients 89794.1 and 89794.2 are brothers; 75898.2 is the daughter of 75898.3 and mother of 75898.1. The genetic and phenotypic findings in 75898.2 and 75898.3 are also discussed in.<sup>15</sup>

The ABC method was then used to produce a set of potential enhancers using default parameters. As described by Fulco et al., initial peaks were obtained using the MACS2 (Model-based Analysis of ChIP-Seq 2) peak caller on aligned ATAC-seq reads with a lenient *P* value using the following options “-g hs, -p .1, -call-summits.”<sup>39</sup> The peaks were then extended by 250 base-pairs from their summits to produce a set of 500 base-pair candidate regions; overlapping regions were then merged. This process resulted in a broad set of potential regulatory elements whose activity could be scored. To accomplish this goal, the ATAC-seq and H3K27ac ChIP-seq reads overlapping each candidate region were counted and averaged over biological replicates using the ABC “call neighborhoods” script. Finally, Hi-C data from human embryonic stem cells were downloaded from the juicebox archive at 5000 base-pair resolution.<sup>25</sup> Averaged Hi-C data provided by the ABC GitHub page were also used; these data were produced by averaging the Hi-C profiles from 10 cell types (GM12878, NHEK, HMEC, RPE1, THP1, IMR90, HUVEC, HCT116, K562, and KBM7). ABC scores were calculated by combining the estimated contact frequency (between the candidate region and the promoter of a gene) with the observed activity using the default parameters.

### Analysis of PRDM13 Gene Expression in the Human Retina

To determine the expression level of *PRDM13*, we used a resource collecting human RNA-seq datasets: eyeIntegration.<sup>40</sup> All retinal tissue subtypes, RPE subtypes, and progenitor subtypes were queried. Because eyeIntegration does not presently contain data on macula, *PRDM13* expression was also estimated from three macula RNA-seq samples included in the GEO dataset GSE137311.<sup>26</sup> In short, the raw reads were quantified using salmon<sup>41</sup> (according to the same protocol used to build the eyeIntegration dataset) and the value in transcripts per million (TPM) was calculated using tximport to merge reads to the gene level with the “length-ScaledTPM” option. The source code for this pipeline can be found at: <https://github.com/davemcg/scEiaD/>. DESCARTES (available at: <https://descartes.brotmanbaty.org/>) was also queried for *PRDM13* expression. Finally, *PRDM13* expression was determined in individual cell types using the plae (Platform for Analysis of scEiaD version 0.43) database (available at: <https://plae.nei.nih.gov/>).

## RESULTS

### Clinical Characteristics of Study Participants

All six study participants were heterozygous for the chr6:100,040,987G>C variant. This change has been detected previously in a number of families segregating NCMD<sup>1,3,4,15</sup> and seemed to be on the same genetic background (haplotype) in at least two of the families included in this study (families 75898 and 89794) (Supplementary Table S1).

The age at presentation of study participants ranged from 3 to 46 years of age and the visual acuity ranged from 0.0 to 1.6 LogMAR. Three related patients presented in the first years of life and had vision of 0.5 LogMAR or worse; the remaining three patients had normal vision and were only found to have drusen-like macular lesions on routine eye tests. The clinical findings are discussed in Table 1, the pedigrees are shown in Figure 1, and fundus imaging results are shown in Figures 2 and 3. The central macular changes resembled fine, confluent drusen; these lesions were hyperautofluorescent on fundus autofluorescence imaging and only partially corresponded to visible OCT changes. A notable finding in all participants was that of characteristic yellow-white drusen-like retinal lesions in the far periphery; these lesions generally had a linear, radial configuration and could be detected on widefield imaging (Fig. 3). The youngest study participant developed choroidal neovascularization in both maculae (diagnosed at 6 years of age). An active lesion was noted in the right eye on OCT-A and treatment with intravitreal bevacizumab injections was initiated. However, persistent subretinal fluid was present after four injections.

### In Silico Analysis of Variants Associated With NCMD

To date, five NCMD-associated single nucleotide variants have been reported in the biomedical literature. These variants were found to be extremely rare upon inspection of large-scale genomic datasets (gnomAD and TOPMed; Table 2). Notably, the chr6:100,040,987G>C change that was detected in the participants of this study was only identified in a single individual in gnomAD; this person was estimated to have European ancestry. None of the five NCMD-associated variants was predicted to be deleterious by CADD. According to nCER, the variants ranged from



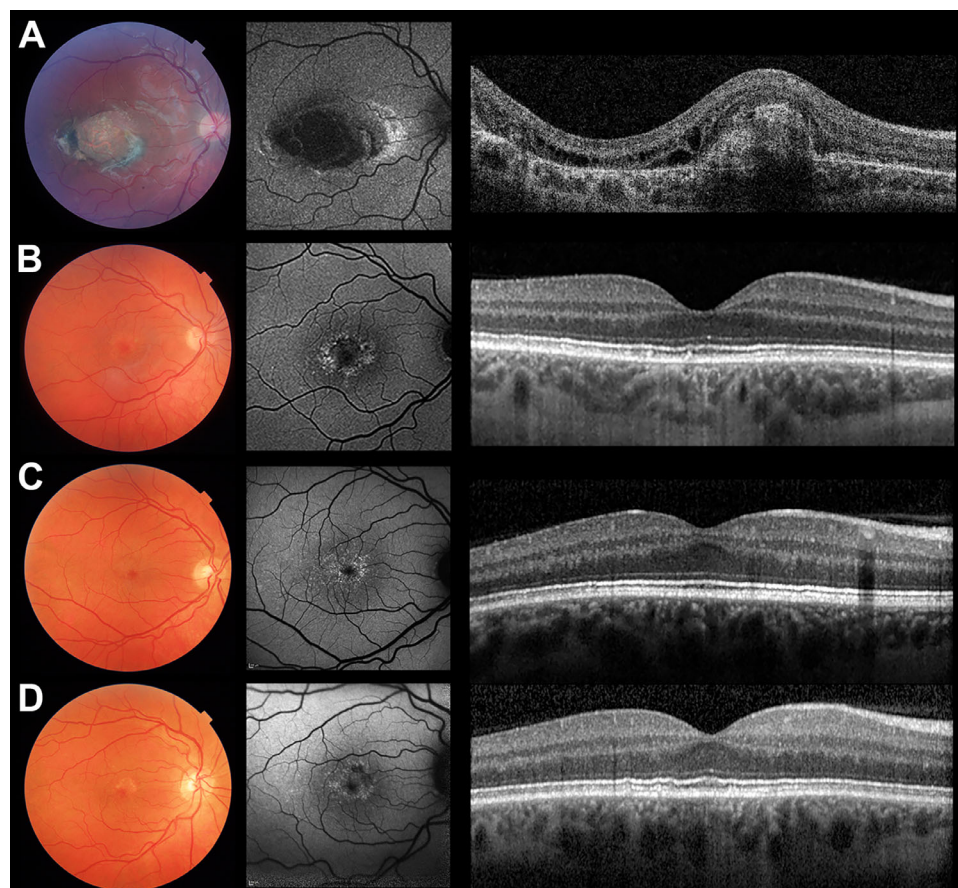


**FIGURE 2.** Color fundus photography, fundus autofluorescence imaging, and OCT from four individuals who have NCMD and are heterozygous for the chr6:100,040,987 variant (GRCh37/hg19). (A) Macular findings in a 6-year-old child are shown. A macular coloboma-like excavation is seen; there is extensive subretinal fibrosis centrally with residual pockets of intraretinal fluid despite treatment with four intravitreal bevacizumab injections. Images of the affected mother and grandmother of this proband can be found in.<sup>15</sup> (B) Macular findings in a 36-year-old proband are shown. Subtle confluent yellow-white specks are noted in the central macula. These are more visible on fundus autofluorescence imaging and correspond with hyperautofluorescent lesions. Only a subset of these changes were readily identifiable by OCT. No inner retinal layer abnormality could be detected. (C, D) Macular findings in a 44-year-old proband and his 48-year-old brother are shown. Yellow-white foveal lesions, similar to those observed in the 36-year-old individual as discussed in (B) are noted. There was a high degree of interocular symmetry and only data from the right eye are shown.

low to middle percentiles.<sup>42</sup> The regBase Phred-like scores ranged from 5.7 to 19.8 on a Phred-like scale from 1 to 99, with higher scores suggesting greater pathogenicity. Inspection of the UniPROBE (Universal PBM Resource for Oligonucleotide Binding Evaluation) database<sup>42</sup> revealed that none of these disease-associated variants is expected to significantly impact on a transcription factor binding site. The GERP scores ranged from  $-2.44$  to  $2.52$ , suggesting variable evolutionary constraint (Table 2).

The degree to which NCMD-associated variants map to putative enhancer elements was then investigated. Two such elements were found in the ENCODE dataset to span the locations of all five disease-associated variants (accessions, EH37E1264999 and EH37E12650011; DNase Z-scores, 3.81 and 1.70). We used the ABC method to assign these enhancers to target genes. Publicly available chromatin accessibility (ATAC-seq and H3K27ac ChIP-seq) datasets from macula and retina were used.<sup>26</sup> The Hi-C data recommended and provided by Fulco et al.<sup>23</sup> were also used; these consist of a Hi-C profile that was averaged over a number of cell types. With this input, ABC did not yield any predictions for the regions spanning the location of NCMD-

associated variants. We then used the same ATAC-seq and H3K27ac ChIP-seq data, but this time combined with Hi-C data from human embryonic stem cells. In macula, two predicted enhancers encompassed the locations of all five variants, and these regions were linked to the *FLH5*, *SIM1*, and *PRDM13* genes.

Because previous reports have associated *PRDM13* with NCMD,<sup>1,2,8</sup> we then looked for enhancer elements predicted to be linked to *PRDM13*. Only elements that were within 100,000 base-pairs of the transcription initiation site were analyzed. This process yielded a total of 53 candidate regions in macular tissue and 47 candidate regions in retinal tissue. To determine which of these candidates have the strongest regulatory effects on *PRDM13*, putative enhancers were ranked according to the overall ABC score and to the individual components of this score (i.e., activity and contact) in isolation. The top 10 predicted elements ranked by their ABC scores are shown in Supplementary Tables S2 and S3.

One previously reported NCMD-associated variant, chr6:100,046,783A>C, fell within a predicted enhancer that spanned approximately the same coordinates in

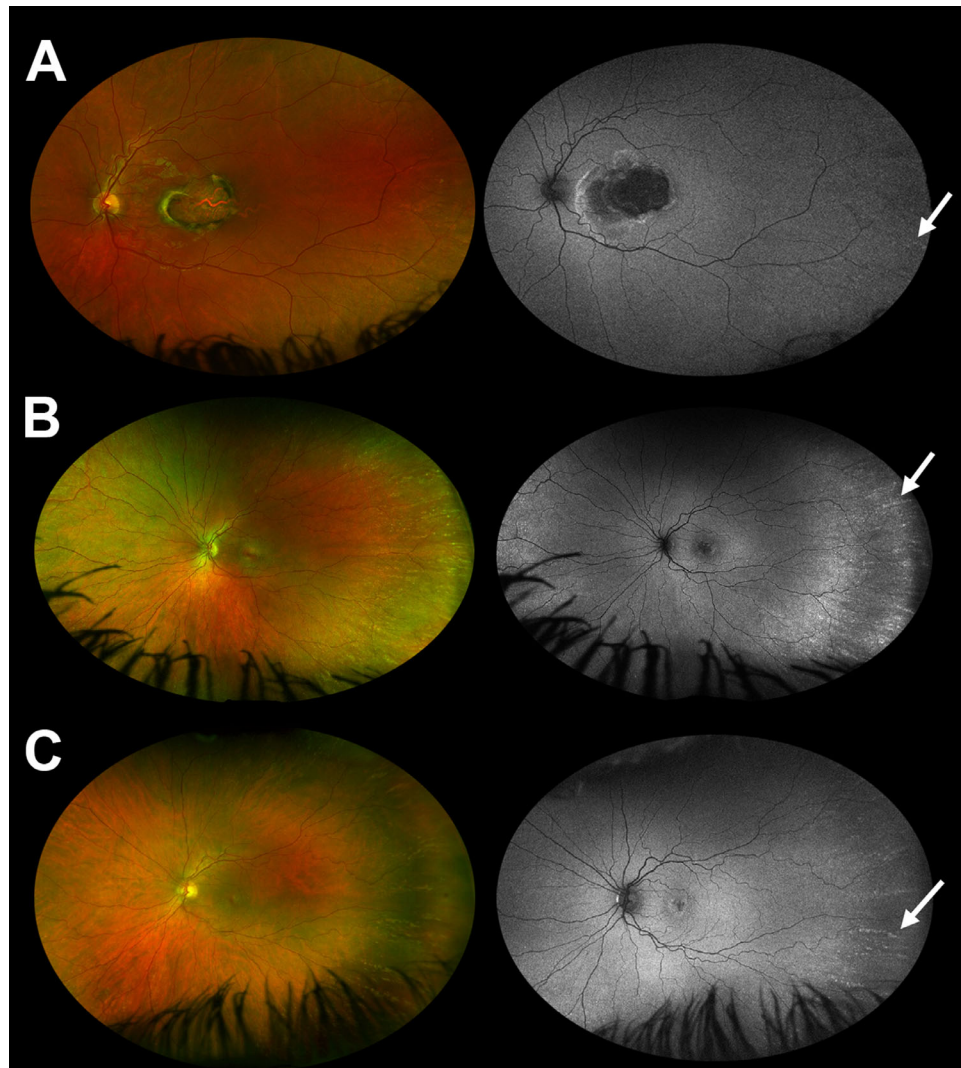


**FIGURE 3.** Digital widefield fundus imaging and fundus autofluorescence imaging in three probands who have NCMD and are heterozygous for the chr6:100,040,987 variant (GRCh37/hg19). Images from a 6-year-old (**A**), a 36-year-old (**B**), and a 48-year-old (**C**) are shown. Yellow-white retinal spots, often very prominent and in radial alignment, are noted in the far temporal periphery of these three individuals. These spots correspond to hyperautofluorescent lesions on fundus autofluorescence imaging. White arrows are used to highlight some of these changes. Inferior lash artefact is noted in some images. There was a high degree of interocular symmetry and only data from the left eye are shown. It is worth noting that although there was significant phenotypic variability, widefield imaging revealed a maculopathy combined with peripheral drusen-like spots in all study participants.

both macula and retina (chr6:100,046,330-100,046,830 and chr6:100,046,348-100,046,848, respectively) (Fig. 4). In terms of ranking, this enhancer had low scores for activity but relatively high scores for Hi-C contact when data from embryonic stem cells were used. Another four variants (chr6:100,040,906G>T, chr6:100,040,974A>C, chr6:100,040,987G>C, and chr6:100,041,040C>T) fell within a predicted enhancer spanning the chr6:100,040,653-100,041,153 region. This enhancer was found in macular tissue but not in retina, and had low scores for activity but relatively high scores for Hi-C contact.

Finally, we could not identify any significant single-tissue eQTLs within any of the enhancer elements found in ENCODE or those predicted by the ABC method. Data from multiple tissues were inspected (including retinal samples from EyeGEx<sup>35</sup>).

### PRDM13 Gene Expression in the Developing and Adult Human Retina

To gain insights into the cellular context in which the *PRDM13* gene product exerts its function, we evaluated the levels of gene expression in a number of relevant tissues (Fig. 5). The expression levels were significantly higher in the retina and macula than in the RPE, with the highest level found in fetal retinal tissue. Analysis of single-cell RNA-seq datasets revealed that *PRDM13* is expressed in progenitor cells (including amacrine/horizontal precursors), with higher expression in the amacrine population. *PRDM13* had low expression levels (<0.2 TPM) in all tissues found in the GTEx project dataset. For further detail on the expression of *PRDM13* across tissues and cell types, see Supplementary Table S4 and Supplementary Figure S1.

TABLE 2. Single Nucleotide Variants in Chromosome 6 Associated With NCMD

Variant (GRCh37/hg19)	Variant (GRCh38/hg38)	gnomAD Allele Count	TOPMed Allele Count	CADD-Phred Score	regBase Score	ncER Percentile	GERP Score	Number of 'Families' (Number of Affected)	Reference
chr6:100,040,906G>T	chr6:99,593,030G>T	0/~152,100	0/~264,690	1.672	19.8	81.33	-0.01	6 (65)	1
chr6:100,040,974A>C	chr6:99,593,098A>C	0/~152,100	0/~264,690	1.465	8.3	73.36	-2.19	1 (6)	9
chr6:100,040,987G>C	chr6:99,593,111G>C	1/152,188	0/~264,690	9.133	19.5	79.83	2.52	14 (41)	1,3,4,15,44
chr6:100,041,040C>T	chr6:99,593,164C>T	0/~151,800	0/~264,690	5.647	16.9	69.37	1.72	1 (2)	1
chr6:100,046,783A>C	chr6:99,598,907A>C	0/~152,100	0/~264,690	2.528	5.7	15.60	-2.44	1 (2)	2

gnomAD, Genome Aggregation Database v3.1 dataset; GERP, Genomic Evolutionary Rate Profiling; TOPMed, NHLBI Trans-Omics for Precision Medicine variant database freeze 8; CADD, Combined Annotation Dependent Depletion; ncER, nonCoding Essential Regulation.

The CADD score ranges from 1 to 99; a higher score indicates greater pathogenicity. Values of 10 or greater are predicted to be the 10% most deleterious substitutions and values of 20 or greater in the 1% most deleterious.

The ncER scores are percentiles. The higher the percentile, the more likely that a region is vital in terms of regulation. There is no agreed cut-off for deleteriousness but the original report focused on assessing the predictive power of the higher percentiles (≥95th).

The regBase scores are Phred-like and calculated using the “PAT” model, which attempts to determine whether a variant is deleterious. The scores range from 1 to 99; a higher score indicates greater pathogenicity.

The GERP scores represent position-specific evolutionary constraint. Positive values suggest evolutionarily constrained positions, with a cut-off of 2 providing high sensitivity.

\* The relevant family described by Silva et al<sup>2</sup> includes a female proband with NCMD and her son who has been noted to have progressive bifocal chorioretinal atrophy (PBCRA). Although the son seems to have a more severe developmental maculopathy than his mother; the clinical information provided in the original report suggests that his phenotype is more in keeping with NCMD than with PBCRA. Notably, a nearby variant, chr6:100,046,804T>C (GRCh37/hg19), has been found to cause PBCRA in six affected individuals from two families (see also Fig. 4).<sup>2</sup>

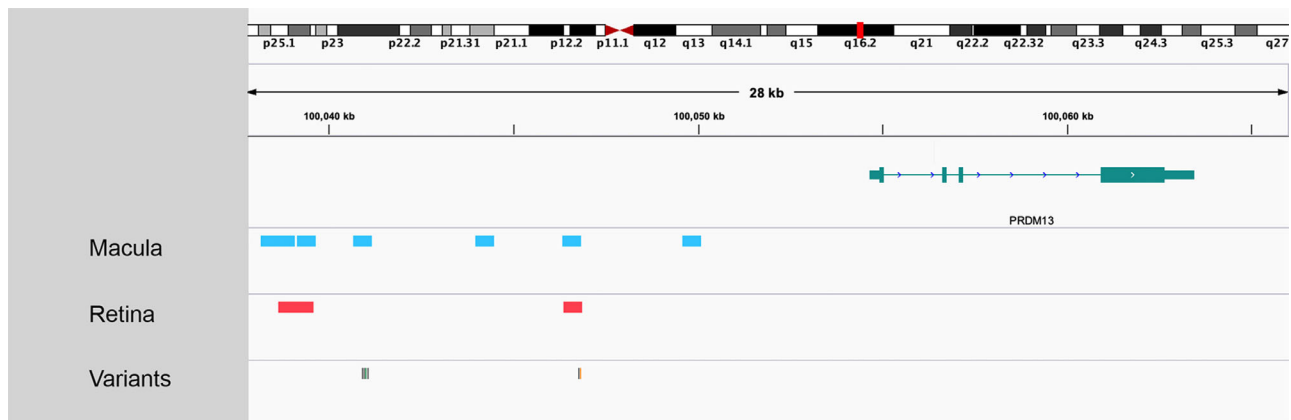


FIGURE 4. Location of enhancer elements upstream of *PRDM13* in macula and retina as predicted by the ABC model.<sup>23</sup> A putative enhancer encompasses the chr6:100,040,987G>C (GRCh37/hg19) variant, which was carried by the six study participants (green line in the variant row). The enhancer encompassing this variant was not detected in retinal tissue and was only highlighted when a dataset from macular tissue was used. This enhancer overall encompasses four variants that were previously identified in families with NCMD: chr6:100,040,906G>T, chr6:100,040,974A>C, chr6:100,040,987G>C, and chr6:100,041,040C>T. A different candidate enhancer that was predicted to be functional in both macular and retinal tissue was altered by the chr6:100,046,783A>C variant. This change has been identified in a single family with two affected individuals, a mother and her son; although the mother had typical findings of NCMD, the child had broader retinal involvement and has been documented to have a related developmental disorder, progressive bifocal chorioretinal atrophy (PBCRA).<sup>2</sup> Notably, an adjacent variant, chr6:100,046,804T>C (orange line in the variant row of the Figure), has been reported to cause PBCRA in six affected individuals from two families.<sup>2</sup> The fact that the candidate enhancer encompassing these two PBCRA-implicated variants appears to have a role in both macular and retinal tissue may explain why individuals carrying these changes can develop a phenotype that is more severe than classical NCMD and is associated with extramacular involvement.

DISCUSSION

In this study, we report clinical and genetic findings from six patients with NCMD. We highlight the usefulness of wide-field retinal imaging in individuals suspected to have NCMD (Fig. 3) and discuss the need for monitoring for choroidal neovascularization, particularly in young affected children. Furthermore, we perform computational analysis of NCMD-associated changes, with the results further supporting the role of *PRDM13* dysregulation in the pathogenesis of the condition.

Phenotypic variability is incompletely understood, but common in NCMD.<sup>1,3</sup> It is therefore not surprising that significant differences in clinical presentation were observed among the participants of this study. It is worth highlighting, however, that the three mildest cases were asymptomatic and were initially incorrectly diagnosed in adulthood as having a form of early onset macular drusen; OCT imaging revealed that these macular changes were unlike typical drusen (Fig. 2) and genetic testing highlighted the congenital nature of these lesions. It is noteworthy that histopathologic examination of an enucleated eye from a 72-year-old



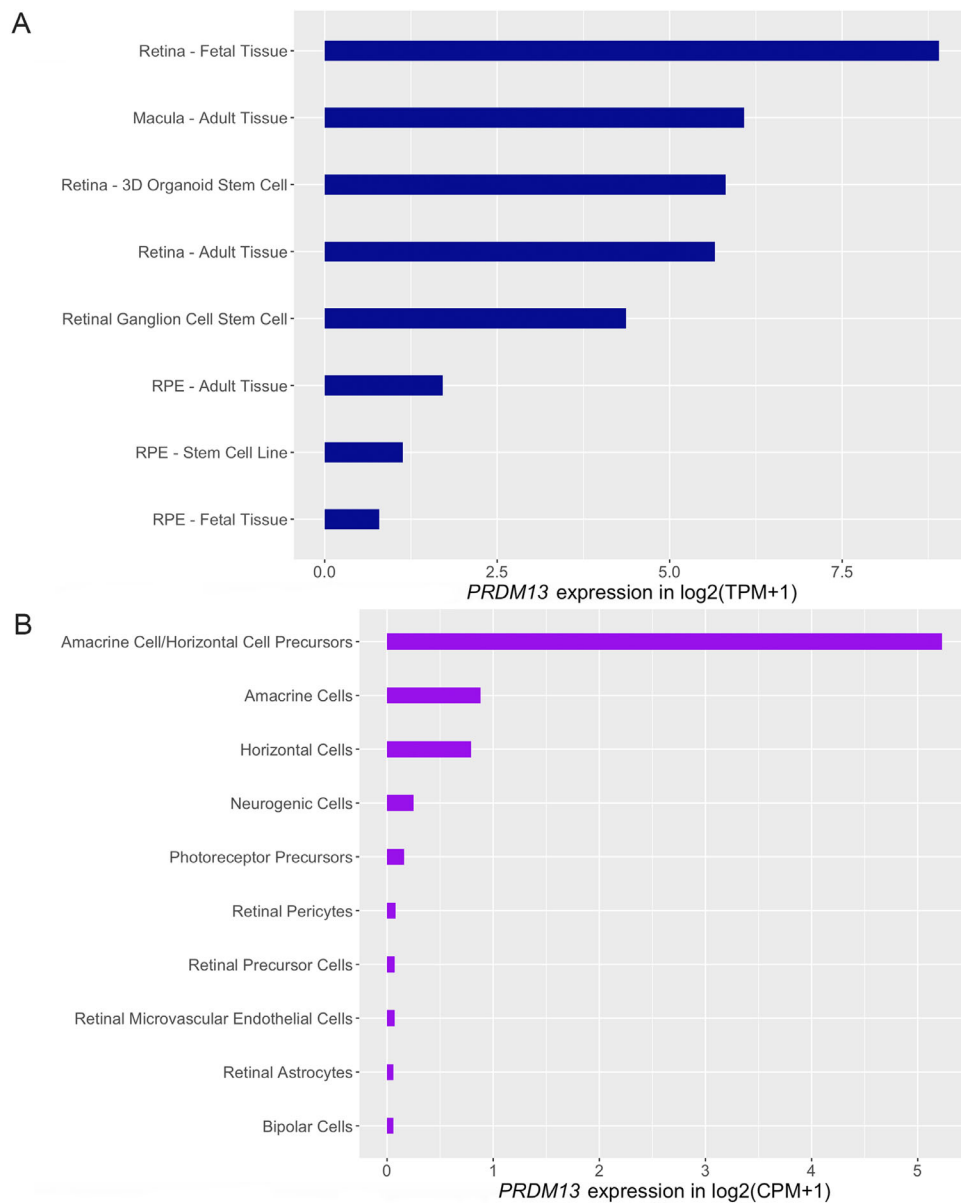


**FIGURE 5.** Expression levels of *PRDM13* in different human tissues and cells. **(A)** Gene expression of *PRDM13* in human tissues from bulk RNA, taken from eyeIntegration (<https://eyeintegration.nei.nih.gov/>, v1.05). **(B)** Gene expression of *PRDM13* in cell populations from single-cell RNA-seq studies (<https://plae.nei.nih.gov/>, v0.43). It is noteworthy that *PRDM13* had very low expression levels (<0.2 TPM) in all extraocular tissues included in the Genotype-Tissue Expression (GTEx) project dataset.<sup>34</sup> TPM, transcripts per million; CPM, counts per million.

patient with a clinical diagnosis of NCMD revealed sub-RPE deposits.<sup>43</sup> However, OCT findings from this and other studies<sup>9</sup> suggest that at least a subset of these lesions may be anterior to the RPE. The most severely affected participant in this study was a 6-year-old male patient who had coloboma-like excavation and subretinal fibrosis in both maculae. Notably, he experienced moderate to severe visual loss owing to the formation of choroidal neovascularization. This is a rare but sight-threatening complication of NCMD that can occur in both children and adults.<sup>1,5,44–46</sup> A previous report has shown that intravitreal bevacizumab injections can improve vision and decrease intraretinal fluid. However, multiple injections (in a treat-and-extend protocol) may be required.<sup>45</sup>

We highlight an under-recognized fundoscopic finding of NCMD: multiple drusen-like spots in the peripheral retina. These lesions were noted in all study participants and were easily detected on widefield retinal imaging (Fig. 3). Although this feature is not pathognomonic, it prompted targeted genetic testing in one of the probands. Similar retinal abnormalities have been previously described in a number of affected families, including in the original NCMD kindred.<sup>5,6,11,44,47,48</sup> These peripheral lesions should, therefore, be sought after in all individuals with a clinical presentation suggestive of NCMD and their presence should provide additional justification for requesting focused genetic screening. Further retinal imaging, including widefield OCT, is expected to provide important insights



into the nature of this common but frequently overlooked feature of NCMD.

Although a number of noncoding genetic variants have been associated with NCMD, our understanding of the molecular pathology of this condition remains incomplete. The recent emergence of comprehensive functional genomic datasets from adult and fetal human tissues<sup>20,21,26</sup> has enabled the in-depth analysis of noncoding changes like the ones implicated in this disorder. We found that all NCMD-associated variants fall within enhancer elements that appear to be active during development and to be linked to the retinal transcription factor *PRDM13*. A number of observations relating to our in silico analysis are worthy of further discussion. First, the candidate enhancer that encompasses chr6:100,040,987G>C, the variant carried by the six study participants, was absent when retina-derived epigenomic data were used and was only highlighted when a dataset from macular tissue was used (Fig. 4). Second, there were stark differences in the computational predictions of the ABC algorithm depending on the type of Hi-C data used as input (averaged/non-tissue-specific vs. embryonic tissue-specific profiles). This finding is notable because the developers of the ABC algorithm concluded that a Hi-C profile generated by averaging over several tissue types performed equally well to tissue-specific data. However, our findings indicate a potential pitfall in using averaged Hi-C data for genes that are most highly expressed during development.

The human retina emerges in three main stages. The early retina is characterized by retinal progenitor proliferation and RPE emergence (5–7 postconception weeks); this period is followed by ganglion cell production and initiation of the programs that underlie the development of horizontal cells, amacrine cells, and cone photoreceptors (7–10 postconception weeks). Subsequently, cone, amacrine, rod, bipolar, and Muller glia cells sequentially emerge (12–18 postconception weeks).<sup>49,50</sup> Interestingly, the morphologic differentiation of the fovea is completed earlier than other regions for all cell types.<sup>49</sup> Our gene expression analyses of human tissues revealed that *PRDM13* is expressed predominantly in the retinal progenitor and the amacrine cell populations. Amacrine cells are the most diverse class of retinal neurons and are often subdivided based on the expression of inhibitory  $\gamma$ -aminobutyric (GABA) or glycine. Studies in animal models have shown that *PRDM13* is a key determinant of amacrine cell fate and promotes the generation of amacrine cell subtypes (with a bias toward a glycinergic phenotype). Given that duplications of the *PRDM13* region are an established cause of NCMD, it has been proposed that over-expression of this gene during development is the main disease mechanism.<sup>16</sup> This is supported by findings in *Drosophila*, *Xenopus*, and murine retinae, although none of these animal models has a macula.<sup>51,52</sup> How impaired amacrine cell specification leads to macular abnormalities remains unclear. It is noteworthy though that the inner retinal layers (including the amacrine cell bodies) seemed to be normal on OCT imaging (Fig. 2). Previous studies have however reported cases with subtle foveal hypoplasia<sup>3</sup> or electrophysiologic findings,<sup>16</sup> suggesting amacrine cell abnormalities. These reports are, however, sporadic and the in-depth phenotyping of more affected individuals will provide further insights.

In conclusion, we have used human transcriptomic and epigenomic datasets to study the disease mechanism of NCMD. We highlight the value of computational approaches for the evaluation of candidate noncoding variants and

discuss the importance of taking spatiotemporal context into account in these analyses. Furthermore, we report a common peripheral retinal finding challenging the notion that NCMD is a disorder strictly confined to the macula.

### Acknowledgments

Supported by the Wellcome Trust (200990/Z/16/Z, Transforming Genetic Medicine Initiative); Christopher Green; Retina UK and Fight for Sight (GR586, RP Genome Project); Health Education England; UK National Institute for Health Research (NIHR) Clinical Lecturer Programme (CL-2017-06-001). Christopher Green Doctoral Fellowship (DJG); UK National Institute for Health Research (NIHR) Clinical Lecturer Award (CL-2017-06-001, PIS); Health Education England Postdoctoral Research Fellowship (JME); Retina UK and Fight for Sight (GR586, RP Genome Project - UK Inherited Retinal Disease Consortium; GCB); Wellcome Trust (200990/Z/16/Z, Transforming Genetic Medicine Initiative; EL, GCB).

Disclosure: **D.J. Green**, None; **E. Lenassi**, None; **C.S. Manning**, None; **D. McGaughey**, None; **V. Sharma**, None; **G.C. Black**, None; **J.M. Ellingford**, None; **P.I. Sergouniotis**, None

### References

- Small KW, Udar N, Ph D, et al. North Carolina macular dystrophy is caused by dysregulation of the retinal transcription factor PRDM13. *Ophthalmology*. 2016;123(1):319–335, <https://doi.org/10.1016/j.ophtha.2015.10.006.North>.
- Silva RS, Arno G, Cipriani V, et al. Unique noncoding variants upstream of PRDM13 are associated with a spectrum of developmental retinal dystrophies including progressive bifocal chorioretinal atrophy. *Hum Mutat*. 2019;40(5):578–587, <https://doi.org/10.1002/humu.23715>.
- Small KW, Tran EM, Small L, Rao RC, Shaya F. Multimodal imaging and functional testing in a North Carolina macular disease family: toxoplasmosis, fovea plana, and torpedo maculopathy are phenocopies. *Ophthalmol Retin*. 2019;3(7):607–614, <https://doi.org/10.1016/j.oret.2019.03.002>.
- Small KW, Vincent AL, Knapper CL, Shaya FS. Congenital toxoplasmosis as one phenocopy of North Carolina macular dystrophy (NCMD/MCDR1). *Am J Ophthalmol Case Reports*. 2019;15:100521, <https://doi.org/10.1016/j.ajoc.2019.100521>.
- Small KW. North Carolina macular dystrophy: clinical features, genealogy, and genetic linkage analysis. *Trans Am Ophthalm Soc*. 1998;96:925–961.
- Small KW. North Carolina macular dystrophy, revisited. *Ophthalmology*. 1989;96(12):1747–1754, [https://doi.org/10.1016/S0161-6420\(89\)32655-8](https://doi.org/10.1016/S0161-6420(89)32655-8).
- Lefler WH, Wadsworth JAC, Sidbury JB. Hereditary macular degeneration and amino-aciduria. *Am J Ophthalmol*. 1971;71(1 Part 2):224–230, [https://doi.org/10.1016/0002-9394\(71\)90394-1](https://doi.org/10.1016/0002-9394(71)90394-1).
- Frank HR, Landers MB, Williams RJ, Sidbury JB. A new dominant progressive foveal dystrophy. *Am J Ophthalmol*. 1974;78(6):903–916, [https://doi.org/10.1016/0002-9394\(74\)90800-9](https://doi.org/10.1016/0002-9394(74)90800-9).
- Namburi P, Khateb S, Meyer S, et al. A unique PRDM13-associated variant in a Georgian Jewish family with probable North Carolina macular dystrophy and the possible contribution of a unique CFH variant. *Mol Vis*. 2020;26(April):299–310.
- Rosenberg T, Roos B, Johnsen T, et al. Clinical and genetic characterization of a Danish family with North Carolina macular dystrophy. *Mol Vis*. 2010;16(June):2659–2668.

11. Reichel MB, Kelsell RE, Fan J, et al. Phenotype of a British North Carolina macular dystrophy family linked to chromosome 6q. *Br J Ophthalmol*. 1998;82(10):1162–1168, <https://doi.org/10.1136/bjo.82.10.1162>.
12. Kiernan DF, Shah RJ, Hariprasad SM, et al. Thirty-Year follow-up of an African American family with macular dystrophy of the retina, locus 1 (North Carolina macular dystrophy). *Ophthalmology*. 2011;118(7):1435–1443.
13. Small KW, Garcia CA, Gallardo G, Udar N, Yelchits S. North Carolina macular dystrophy (MCDR1) in Texas. *Retina*. 1998;18(5):448–452.
14. Small KW, Weber JL, Roses A, et al. North Carolina macular dystrophy is assigned to chromosome 6. *Genomics*. 1992;13:681–685, [https://doi.org/10.1016/0888-7543\(92\)90141-E](https://doi.org/10.1016/0888-7543(92)90141-E).
15. Ellingford JM, Sergouniotis PI, Jenkins E, Black GC. Genome sequencing identifies a non-coding variant in the MCDR1 locus as a cause of macular dystrophy. *Clin Experiment Ophthalmol*. 2017;45(3):297–299, <https://doi.org/10.1111/ceo.12825>.
16. Manes G, Joly W, Guignard T, et al. A novel duplication of PRMD13 causes North Carolina macular dystrophy: overexpression of PRDM13 orthologue in drosophila eye reproduces the human phenotype. *Hum Mol Genet*. 2017;26(22):4367–4374, <https://doi.org/10.1093/hmg/ddx322>.
17. Bhatia S, Bengani H, Fish M, et al. Disruption of autoregulatory feedback by a mutation in a remote, ultraconserved PAX6 enhancer causes aniridia. *Am J Hum Genet*. 2013;93(6):1126–1134, <https://doi.org/10.1016/j.ajhg.2013.10.028>.
18. Vandermeer JE, Ahituv N. Cis-regulatory mutations are a genetic cause of human limb malformations. *Dev Dyn*. 2011;240(5):920–930, <https://doi.org/10.1002/dvdy.22535>.
19. Gasperini M, Tome JM, Shendure J. Towards a comprehensive catalogue of validated and target-linked human enhancers. *Nat Rev Genet*. 2020;21:292–310, <https://doi.org/10.1038/s41576-019-0209-0>.
20. Abascal F, Acosta R, Addleman NJ, et al. Expanded encyclopaedias of DNA elements in the human and mouse genomes. *Nature*. 2020;583(7818):699–710, <https://doi.org/10.1038/s41586-020-2493-4>.
21. Domcke S, Hill AJ, Daza RM, et al. A human cell atlas of fetal chromatin accessibility. *Science*. 2020;370(6518):eaba7612, <https://doi.org/10.1126/science.aba7612>.
22. Cao J, O'Day DR, Pliner HA, et al. A human cell atlas of fetal gene expression. *Science*. 2020;370(808):eaba7721, <https://doi.org/10.1126/science.aba7721>.
23. Fulco CP, Nasser J, Jones TR, et al. Activity-by-contact model of enhancer–promoter regulation from thousands of CRISPR perturbations. *Nat Genet*. 2019;51(12):1664–1669, <https://doi.org/10.1038/s41588-019-0538-0>.
24. Nasser J, Bergman DT, Fulco CP, et al. Genome-wide enhancer maps link risk variants to disease genes. *Nature*. 2021;593(7858):238–243, <https://doi.org/10.1038/s41586-021-03446-x>.
25. Dixon JR, Jung I, Selvaraj S, et al. Chromatin architecture reorganization during stem cell differentiation. *Nature*. 2015;518(7539):331–336, <https://doi.org/10.1038/nature14222>.
26. Cherry TJ, Yang MG, Harmin DA, et al. Epigenomic profiling and single-nucleus-RNA-Seq reveal cis-regulatory elements in human retina, macula and RPE and non-coding genetic variation. *bioRxiv*. 2018:412361, <https://www.biorxiv.org/content/10.1101/412361v1.full>.
27. de Bruijn SE, Fiorentino A, Ottaviani D, et al. Structural variants create new topological-associated domains and ectopic retinal enhancer-gene contact in dominant retinitis pigmentosa. *Am J Hum Genet*. 2020;107(5):802–814, <https://doi.org/10.1016/j.ajhg.2020.09.002>.
28. Karczewski KJ, Francioli LC, Tiao G, et al. Variation across 141,456 human exomes and genomes reveals the spectrum of loss-of-function intolerance across human protein-coding genes. *bioRxiv*. 2019:531210, <https://doi.org/10.1101/531210>.
29. Zachary A, Torres R, Taliun SAG, et al. Sequencing of 53 , 831 diverse genomes from the NHLBI TOPMed Program. *bioRxiv*. 2019:563866.
30. Rentzsch P, Witten D, Cooper GM, Shendure J, Kircher M. CADD: Predicting the deleteriousness of variants throughout the human genome. *Nucleic Acids Res*. 2019;47(D1):D886–D894, <https://doi.org/10.1093/nar/gky1016>.
31. Wells A, Hecherman D, Torkamani A, et al. Ranking of non-coding pathogenic variants and putative essential regions of the human genome. *Nat Commun*. 2019;10(1):5241, <https://doi.org/10.1038/s41467-019-13212-3>.
32. Zhang S, He Y, Liu H, et al. regBase: whole genome base-wise aggregation and functional prediction for human non-coding regulatory variants. *Nucleic Acids Res*. 2019;47(21):e134, <https://doi.org/10.1093/nar/gkz774>.
33. Cooper GM, Stone EA, Asimenos G, Green ED, Batzoglou S, Sidow A. Distribution and intensity of constraint in mammalian genomic sequence. *Genome Res*. 2005;15(7):901–913, <https://doi.org/10.1101/gr.3577405>.
34. The Genotype Tissue Expression (GTEx) Consortium. The GTEx Consortium atlas of genetic regulatory effects across human tissues. *bioRxiv*. 2019:787903, <https://doi.org/10.1101/787903>.
35. Ratnapriya R, Sosina OA, Starostik MR, et al. Retinal transcriptome and eQTL analyses identify genes associated with age-related macular degeneration. *Nat Genet*. 2019;51(4):606–610, <https://doi.org/10.1038/s41588-019-0351-9>.
36. Chen S, Zhou Y, Chen Y, Gu J. Fastp: an ultra-fast all-in-one FASTQ preprocessor. *Bioinformatics*. 2018;34(17):i884–i890, <https://doi.org/10.1093/bioinformatics/bty560>.
37. Langmead B, Salzberg SL. Fast gapped-read alignment with Bowtie 2. *Nat Methods*. 2012;9(4):357–359, <https://doi.org/10.1038/nmeth.1923>.
38. Li H, Handsaker B, Wysoker A, et al. The sequence alignment/map format and SAMtools. *Bioinformatics*. 2009;25(16):2078–2079, <https://doi.org/10.1093/bioinformatics/btp352>.
39. Gaspar JM. Improved peak-calling with MACS2. *bioRxiv*. 2018:496521, <https://doi.org/10.1101/496521>.
40. Swamy V, McGaughey D. Eye in a disk: eyeIntegration human pan-eye and body transcriptome database version 1.0. *Invest Ophthalmol Vis Sci*. 2019;60(8):3236, <https://doi.org/10.1167/iovs.19-27106>.
41. Evans E. Salmon: fast and bias-aware quantification of transcript expression using dual-phase inference. *Midwives Chron*. 1972;86(11):118–119, <https://doi.org/10.1038/nmeth.4197.Salmon>.
42. Hume MA, Barrera LA, Gisselbrecht SS, Bulyk ML. UniPROBE, update 2015: new tools and content for the online database of protein-binding microarray data on protein-DNA interactions. *Nucleic Acids Res*. 2015;43(D1):D117–D122, <https://doi.org/10.1093/nar/gku1045>.
43. Voo I, Glasgow BJ, Flannery J, Udar N, Small KW. North Carolina macular dystrophy: clinicopathologic correlation. *Am J Ophthalmol*. 2001;132(6):933–935, [https://doi.org/10.1016/S0002-9394\(01\)01184-9](https://doi.org/10.1016/S0002-9394(01)01184-9).
44. Birtel J, Gliem M, Herrmann P, et al. North Carolina macular dystrophy shows a particular drusen phenotype and atrophy progression. *Br J Ophthalmol*. 2021

- Mar 30 [Epub ahead of print], <https://doi.org/10.1136/bjophthalmol-2021-318815>.
45. Bakall B, Bryan JS, Stone EM, Small KW. Choroidal neovascularization in North Carolina macular dystrophy responsive to anti-vascular endothelial growth factor therapy. *Retin Cases Brief Rep*. 2018 Oct 31 [Epub ahead of print], <https://doi.org/10.1097/icb.0000000000000838>.
  46. Rhee DY, Reichel E, Rogers A, Strominger M. Subfoveal choroidal neovascularization in a 3-year-old child with North Carolina macular dystrophy. *J AAPOS*. 2007;11(6):614–615, <https://doi.org/10.1016/j.jaapos.2007.06.010>.
  47. Pauleikhoff D, Sauer CG, Muller CR, Radermacher M, Merz A, Weber BHF. Clinical and genetic evidence for autosomal dominant North Carolina macular dystrophy in a German family. *Am J Ophthalmol*. 1997;124(3):412–415, [https://doi.org/10.1016/S0002-9394\(14\)70842-6](https://doi.org/10.1016/S0002-9394(14)70842-6).
  48. Small KW, Killian J, McLean WC. North Carolina's dominant progressive foveal dystrophy: how progressive is it? *Br J Ophthalmol*. 1991;75(7):401–406, <https://doi.org/10.1136/bjo.75.7.401>.
  49. Hoshino A, Ratnapriya R, Brooks MJ, et al. Molecular anatomy of the developing human retina. *Dev Cell*. 2017;43(6):763–779.e4, <https://doi.org/10.1016/j.devcel.2017.10.029>.
  50. Mellough CB, Bauer R, Collin J, et al. An integrated transcriptional analysis of the developing human retina. *Dev*. 2019;146(2):dev169474, <https://doi.org/10.1242/dev.169474>.
  51. Bessodes N, Parain K, Bronchain O, Bellefroid EJ, Perron M. Prdm13 forms a feedback loop with Ptf1a and is required for glycinergic amacrine cell genesis in the Xenopus retina. *Neural Dev*. 2017;12(1):1–15, <https://doi.org/10.1186/s13064-017-0093-2>.
  52. Watanabe S, Sanuki R, Sugita Y, et al. Prdm13 regulates subtype specification of retinal amacrine interneurons and modulates visual sensitivity. *J Neurosci*. 2015;35(20):8004–8020, <https://doi.org/10.1523/JNEUROSCI.0089-15.2015>.